

Controlled Magnet Excitation for Electron Beam Scanning in Industrial Irradiators

B.F. White, S.T. Craig, V.A. Mason, S.M. Morsink* and D.L. Smyth
Atomic Energy of Canada Limited, Research Company
Chalk River Nuclear Laboratories, Chalk River, Canada
*University of Waterloo, Physics Dept., Waterloo, Canada

Abstract

Industrial irradiators based on electron accelerators require that the beam power be distributed over the product exposure plane consistent with the process requirements. In practice, this is achieved by either a static lens system, or magnetic scanning. For the IMPELA™ pulsed irradiators, either a low-frequency (5 Hz) scanner places spots across the product plane or a high-frequency (250 Hz) macro-pulse scanner will sweep each beam pulse across the plane. The performance of both spot and macro-pulse scanners is enhanced by modifying the magnet excitation to compensate for systematic effects, including hysteresis and eddy currents. Synchronous detection of the beam at the edges of the scan pattern is applied to closed-loop control of both the scan width and centroid. Thermal measurements of power distribution with a real-time exposure-dose monitor show beam utilization efficiencies of 85% are achieved relative to a uniform distribution, neglecting scattering.

Introduction

IMPELA™-10/50 is the 10 MeV 50 kW member of a family of industrial irradiators based on electron linear accelerators developed by Atomic Energy of Canada Limited. These accelerators are built from modular, standing-wave structures, operate in a long-pulse mode, and use a low-injection-voltage triode gun. The accelerator is powered with a single, modulated-anode, 1.3 GHz klystron [1]. The rf system provides closed-loop control of the accelerating field during the pulse. The accelerated-beam current is measured and averaged over a number of pulses. The gun emission is adjusted to control the current with the loop closed by the programmable logic controller (PLC) software. Linear (0°) and 270°-bending beam delivery systems have been designed. The beam delivery designs include static and dynamic means to distribute the irradiator power over the product exposure plane [2]. A prototype has been built in the 0° configuration with analytical elements in the beam delivery system, as shown in Figure 1. It has been operational for just over one year. Tests have demonstrated sustained operation at the full 10 MeV energy and 50 kW average beam power.

The power distribution at the product exposure plane must be matched to the needs of the irradiation process. Products are sensitive to factors such as maximum and minimum radiation dose, and scattering effects. This paper describes how prescribed product exposure conditions can be assured with the aid of on-line monitoring.

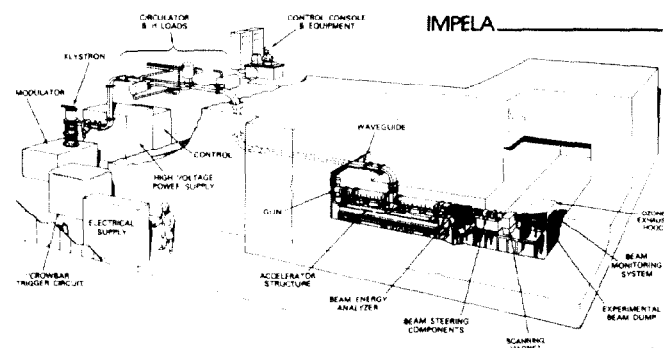


Figure 1. Artist's View of the IMPELA-10/50 Prototype

Dose Uniformity Requirements

Requirements for dose uniformity in a particular product may demand processing with two-sided irradiation, the addition of external scattering surfaces to reduce edge-effects, or the addition of a material layer to modify the depth-dose characteristics of the product. The Quality Assurance (QA) for each product requires a dose assurance protocol. Achieving QA and economy of operation with a minimum of false alarms demands good performance of the dosimetry devices and optimal adjustment of the process conditions. The radiation power-density uniformity specification for the IMPELA™ prototype is $\pm 5\%$, measured at 15 cm from the vacuum window over a width of 80 cm. The portion of the total beam power that falls within this range is $\geq 85\%$.

Magnetic Beam-Deflection

Static or dynamic magnetic systems may be used to distribute the electron beam power over the product exposure plane. While a static lens system can, in principle, achieve a controlled de-focusing of the beam to provide a uniform beam power distribution, achieving this in practice requires a careful design using detailed knowledge of the beam energy spectrum and emittance. Dynamic magnetic scanners may use either a slowly changing magnetic field that places overlapping beam spots at the exposure plane (a spot scanner), or a faster system that slews each beam spot across the plane (a macro-pulse scanner). A spot scanner is operational on the prototype accelerator and a macro-pulse scanner is under development. Both a static system and a macro-pulse scanner offer a lower minimum dose than can be delivered with a spot scanner, while providing a specified uniformity.

Most spot scanners use a deflection electromagnet excited by a current-mode amplifier programmed to follow a triangle wave. Depending on the geometry, at very low frequencies (up to 1 Hz) these scanners use an iron magnetic circuit. As the scan frequency is increased, eddy-currents in the magnet (and to a lesser extent in the vacuum vessel walls) modify the magnet response relative to the zero-frequency hysteresis response. These frequency-dependent effects act to deform the magnetic induction waveform relative to the winding current waveform, producing a non-uniform scanned-beam power distribution with peaks at the ends of the scan pattern.

To improve the performance of a spot scanner, the magnetic circuit may be formed from laminations or ferrites, increasing the effective electrical resistance, and thus reducing eddy-current effects. An alternative that allows use of a simple soft-iron magnetic circuit for intermediate scanning frequencies has been developed for IMPELA™. The scan magnet winding current waveform is deformed to compensate for the eddy-current effects. This approach increases the power dissipated in the iron; however, calculations of the temperature rise predict that only small changes will occur to the permeability and conductivity due to hysteresis and eddy-dissipation. Closed-loop control of the scan width and centroid will minimize changes to the scanned-beam power density.

Characterization of a Scan Magnet

The IMPEIA™-10/50 prototype spot-scan magnet response to sinusoidal current excitation was measured as a function of frequency over the band of 1 to 50 Hz. The magnet was modelled using Maxwell's equations as a simple cylindrical solenoid of equivalent cross-sectional area. The time-dependence of the induction was reduced to the form:

$$G = \exp\left[\frac{r}{2} \left\{ \frac{1}{r^4} - (1 + [P \cdot f]^2)^{0.25} \cos\left(-\frac{1}{2} \text{atan}(P \cdot r^2 \cdot f)\right) \right\}\right] \dots (1),$$

$$\text{and } \theta = \text{atan}\left[G(1 - G^2)^{-0.5} \right] - \frac{\pi}{2} \dots (2), \text{ where}$$

$G = \text{gain}$, $P = \frac{8\pi\mu X}{\rho N N}$, $X = \frac{\text{length}}{N}$, $f = \text{frequency [Hz]}$,

$\theta = \text{phase lag}$, $r = \text{radius}$, $\mu = \text{permeitivity}$, and $\rho = \text{permeability}$.

The response data were fitted to this function, as shown in Figure 2, using X/N as the fitting parameter. To test the extrapolation of the function beyond the frequencies measured, a prediction of the response to a triangle wave current was synthesized. The response function was applied to the closed-form discrete fourier transform (DFT) components of a triangle wave and the induction waveform was synthesized by performing the inverse DFT. The resulting waveform shown in Figure 3 (a), is a reasonable facsimile of the measured magnet-response to a triangle current waveform.

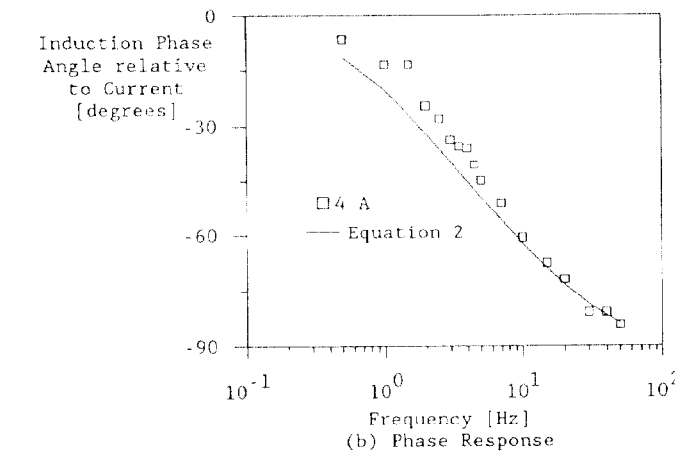
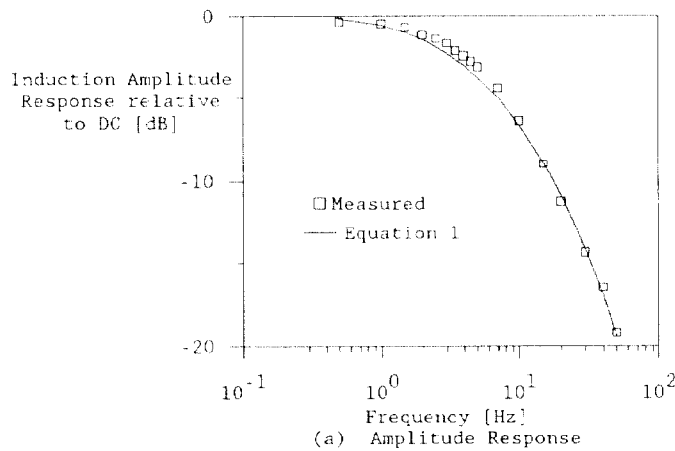


Figure 2. Spot-Scan Magnet Induction

To deliver an arbitrary exposure-plane power-density, an induction waveform may be specified using beam transport models. The process used to model the triangle wave response is then inverted to prescribe the current waveform needed to generate the specified induction. The procedure requires computing the DFT of the desired induction

waveform, applying the inverse of the response function, and computing the inverse DFT to synthesize the current waveform. However, the inverse response function has a gain that increases without bound with increasing frequency. This is not acceptable for a DFT synthesis unless the product of the inverse response function with the component amplitudes reduces toward the nyquist frequency. A modification of the response function (a filter applied in frequency space) is necessary to generate a useful result. Simple filters that limit the amplitude gain were found to be effective.

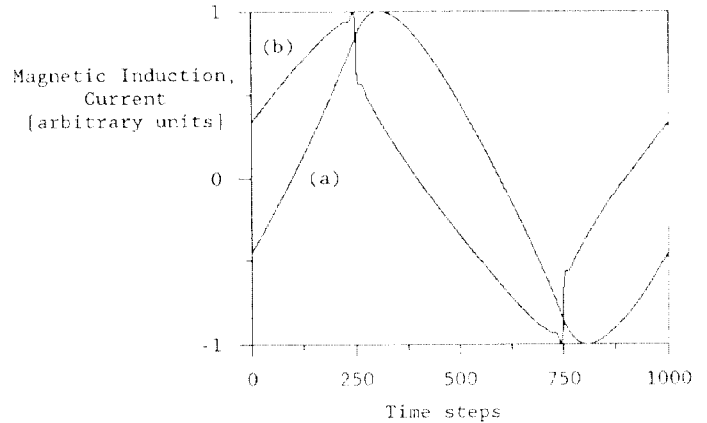


Figure 3. Spot-Scan Magnet
(a) Induction due to Triangle Current
(b) DFT Synthesized Current for Triangle Induction

A sample current waveform synthesized with this method using 10^3 points for 5 Hz is plotted in Figure 3 (b). Beam power distribution measurements made with such waveforms demonstrate that the method is successful in improving the uniformity. Inspection of the prescribed current waveform shapes shows evidence of artifacts due to: (i) the limited bandwidth, and (ii) the time-reversibility implicit with the DFT. These artifacts, which are not consistent with physical intuition, compromise magnet excitation by requiring additional drive power to the reactive load. These waveforms do not produce the optimum uniformity.

By examining the prescribed current waveforms, it is possible to develop guidelines for simpler models. Such a model has been used to generate empirical waveforms that improve scanning performance. These empirical waveforms permit adjusting the balance between the "peaking" at the ends of the power distribution and the "flatness" through the middle. In principle, a custom waveform could be developed to optimize the scanned-beam power distribution for a process.

Feedback Stabilization of the Scan Pattern

On high-power linacs, monitors of the beam position at the end of the scan must be either physically small or cooled to remove the intercepted beam power. Self-powered flux detectors (SPFD) are well-known for monitoring photon fields in reactor applications and may be extended to accelerator-based electron irradiators [3]. These robust detectors operate as simple electronic range-finding probes that are introduced into the edges of the scanning pattern. For our application, Inconel-sheathed, MgO-insulated, tungsten centre-conductor SPFD have been used. The centre-electrode is nearly fully stopping for the incident 10 MeV electrons, and acts as a negative-current source when struck with the high-energy beam. The sheath and insulator provide limited rejection of low-energy electrons (neglecting secondary emission) and a self-shielding geometry for electromagnetic interference.

Macro-pulse Scanner

To sense the edge of the scan pattern, the signal-conditioning electronics sample during each beam pulse over the interval that the beam is approaching the probe. A digital comparator stores the maximum value detected for each scan half-cycle. This value is transferred to the PLC for processing. A fully synchronous scanner is possible; however this would produce a stable, rippled dose-uniformity pattern. Since the spot scanner and the beam pulse are asynchronous, beating effects occur. This beat frequency must be considered in the design of the PLC closed-loop control parameters to ensure stable operation.

Scanned-Beam Power Distribution Thermal Monitor

An array of 23 fully stopping, water-cooled, solid copper rods, instrumented at their mid-points with type J thermocouples, has been used to monitor the scanned-beam power distributions with the IMPELATM-10/50 prototype. The rod temperatures and the cooling manifold inlet temperature are sampled by a scanning data logger and telemetered to an IBM-PC via an RS-232 link. The data are acquired, displayed in real time, and logged to disk with a BASIC-language program. Subsequently, the data are analyzed with a spreadsheet.

The relative temperature rises of the rods provide a direct monitor of the scanned-beam power distribution. To prevent damaging the present apparatus, the accelerator has been operated at reduced average powers of up to 20 kW when the array is installed. Operation at reduced power has been achieved with a shortened beam current pulse length. This maintains the pulse repetition frequency and beam energy corresponding to full power, providing the same uniformity with the spot scanner at 10 kW as delivered at 50 kW.

Scanned-beam power distributions measured on the IMPELATM-10/50 prototype using the triangle wave, DFT synthesized wave, and an empirical waveform are plotted in Figure 4. Since the power distribution monitor has limited spatial resolution, maxima of a distribution may be located by shifting the scanning waveform with an offset. The integral of the area under the curve is a measure of the beam power. For the three distributions shown, the total power estimates obtained by summing the 23 temperature rises are within $\pm 1\%$. These data were collected over a period of several hours, with accelerator operation interrupted to change the waveforms. The area under the end portions where the uniformity falls out of specification corresponds to less than 15% of the total for the modified scan drive waveforms.

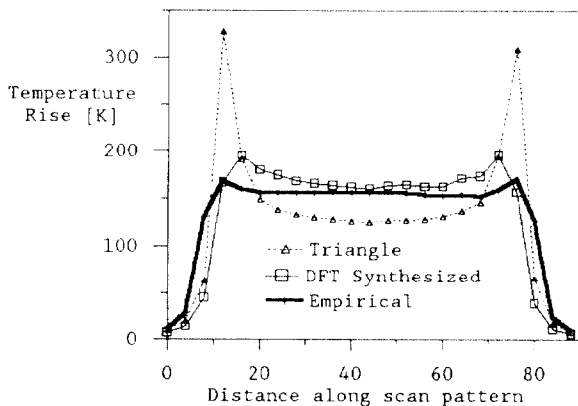


Figure 4. Scanned-Beam Power Distribution

A macro-pulse magnetic scanner could be excited by a transient pulse generator driving a resonant circuit, as a self-resonant circuit with a drive amplifier, or as a tuned-load driven on-resonance by a programmed-current amplifier. A pulsed irradiator must have the accelerator operation synchronized to the macro-pulse scanner with high precision. Otherwise, dose uniformity could suffer, and in the extreme, a high-power irradiator could be damaged by a misplaced beam.

A resonant macro-pulse scan system synchronizes the beam pulse to the time interval near the zero-crossing of the current waveform. For this region, the deviation of the sinusoidal current from a linear ramp limits the useful range to approximately $\pm 38^\circ$ for a $+0\%$, -5% error in the induction. Moreover, for the IMPELATM-10/50 prototype, if the scanner frequency equals a pulse repetition frequency (PRF) of 250 Hz, the phase window for a 200 μ s pulse length corresponds to $\pm 9^\circ$. As a consequence, the peak current in the magnet circuit is 6.4 times that used to deflect the beam to the largest angle. If the scan frequency is a higher harmonic of the PRF (or the pulse length is greater), the phase window is greater and the peak amplitude is reduced.

In a manner analogous to the spot-scan magnet-response characterization and compensated-drive synthesis described above, there are opportunities to develop other macro-pulse scan drive options. For example, the error obtained by synthesizing a triangle wave with only the first three DFT components is less than $\pm 5\%$ for $\pm 88^\circ$. Having developed a sinewave response for a macro-pulse scan magnet and vacuum assembly, the amplitude and phase of each frequency component may be compensated. A suitable current waveform may be synthesized.

If the magnet circuit is series-tuned to be resistive at the fundamental, the reactive impedance at the harmonics will make the current-source-amplifier requirements untenable. However, if the magnet is tuned with a more complex circuit arranged to have a resistive impedance at each of the three frequencies, one may simplify the drive problem. Such a system has advantages for long-pulse operation approaching cw. This approach will be evaluated for the IMPELATM macro-pulse scanner being developed.

Summary

The scanned-beam power distribution of a high-power industrial irradiator has been improved by controlled magnet excitation. This development has been facilitated by on-line monitoring of the distribution. These methods may be applied to optimize the distribution for irradiation processing requirements. Related approaches are being considered in the development of a macro-pulse scanner.

Acknowledgements

The authors acknowledge the contributions made to this work by R.W. Davis, J. McKeown and M.P. Simpson.

References

- [1] J. Ungrin, N.H. Drewell, N.A. Ebrahim, J-P. Labrie, C.B. Lawrence, V.A. Mason, B.F. White, "IMPELA: An Industrial Accelerator Family", 1988 EPAC Conference Proceedings, World Scientific, (1989) 1515-1517.
- [2] V.A. Mason and R.W. Davis, "Beam Delivery Systems for Industrial Accelerators", 1988 Linear Accelerator Conference Proceedings, CEBAF, Va. (1989) 553-555.
- [3] J. McKeown and R.T. Jones, "Important Aspects of Linac Beams for Food Irradiation", NIM, B24/25 (1987) 976-981.